Mathematical Modeling and Simulation for Origami Tsunami Pod

Eri NAKAYAMA, Takamichi SUSHIDA and Ichiro HAGIWARA

Abstract.   Tsunami is caused by a large coastal earthquake. Spherical tsunami shelters were developed in order to avoid serious damages by tsunami. In this paper, we develop the three dimensional model named tsunami pod as a triangulated ellipsoid which can be folded flatly, conduct the numerical simulation by FEM software, and confirm the safety by the von Mises Equivalent value and Head Injury Criterion (HIC). As the result of the first simulation, it is proven that the initial model is weak to the impact force from rigid wall and obstacles and can be strained in the central part. On the other hand, an occupant hits against the internal wall and can be injured. So, the seat and upper and lower bars are added to the initial model. The von Mises equivalent value for the modified model is decreased, however is still over the one of the first simulation. While, HIC value is decreased largely which is much less than the HIC safety level. This is because an occupant does not hit on the internal wall for the occupant restraint system. Moreover, we optimize the form and property for the tsunami pod by minimizing its weight. Finally, we confirm the validity of the optimal model in the original condition of fluid-structure coupling analysis.

1.   Introduction

In the Tohoku earthquake which occurred on March 11 of 2011, serious damages were caused by the tsunami after its earthquake. According to the survey of the Metropolitan Police Department of March 10 of 2015, $15,893$ dead people, $6,152$ injured people, and $2,572$ missing people were confirmed. Since the earthquake, how to protect people's lives from tsunami has been a big issue in Japan. The height of tsunami on land is the same as the several levels of buildings, and its speed is fast as an adult runs with full effort. It is assumed that the broken evacuation route would prevent people from moving, so elder people, disabled people, seriously injured people, and visitors would not easily evacuate to some higher places. As a result of that, they would be drowned and injured severely by obstacles. Recently, as a countermeasure for minimizing the damage occurred by a tsunami, an evacuation building and a floating type shelter have been proposed. These facilities are limited to an urgent and temporary use out of sheer necessity. The spherical shaped shelter which has evacuation space in an upper part and weight and saving space in a lower part was proposed by Shigematsu [**7, 8**]. And, its motion characteristics was examined under hydraulic experiment applying

a reduced model. However, neither experiment nor simulation for examining the motion of an occupant has never been conducted by them. For upgrading to the level of necessities from temporary evacuee facilities, it is essential to consider the performance of storage and conveyance with ensuring safety. As possible solution for storage, foldable structure is considered and an ellipsoid body is applied as its form. This structure is named as "tsunami pod", because the form looks like a shell wrapping bean. For practical applications of this tsunami pod, it is necessary to examine the mechanism to be restrained after being the deployed situation from the folded situation similar to a space antenna, however we will leave the problem as future work.

In this paper, under the condition of coupling phenomenon between structure and fluid, we optimize the design to prevent a tsunami pod from being broken in hitting against rigid walls and obstacles while reducing its weight, and also examine modeling and simulation for design specification to prevent an occupant head from being injured by hitting against the internal side of a tsunami pod.

Product name	Life Amour	HIKARi	Nore	Super Barrier S4
Manufacturing company company	Pond Co., Ltd.	Hikari Rezin Co., Ltd.	Shelter JAPAN Co., Ltd.	World Net International Co., Ltd.
Form on sale	Integrated	Integrated or Assembly	Integrated	Integrated
Material	CFRP	CFRP	CFRP	Steel
Form in use	Spherical body	Spherical body	Spherical body	Dotriacontahedron
Diameter	120 cm	120 cm	120 cm	$180cm$
Weight	80 kg	80 kg	80 kg	500 kg
Maximum number of occupants	4	4	4	6
Withsand load	9 t	22.4 t	12.5 t	
Price	$400,000$ yen	$500,000$ yen	$670,000$ yen	$2,600,000$ yen
Product photo				

Table 1. Commercially available tsunami shelters.

2.   Mathematical modeling for commercially available tsunami pod

2.1.   Consideration of commercially available tsunami shelters

Since the Tohoku earthquake, several kinds of tsunami shelters made of carbon fiber reinforced plastic (CFRP) have been produced by Japanese companies. Table 1 shows those specifications for 4 kinds of tsunami shelters. Concerning form, 3 of them are sphere and one of them is semi-regular dotriacontahedron. The spherical form is assumed to avoid the crash by obstacles and pressure from outside for its curved surface and to be able to diffuse the stress. As a result, it can decrease the load at each point, and suppress the explosion and damage to the utmost limit. CFRP applied into each product as material is a kind of plastic into which epoxy resin is poured to enhance strength not to be bent and crushed. It has superior

characteristics that it is 10 times stronger than iron and one-fifth in weight as the one. It has a good heat retaining property to prevent an occupant from heat and cold, and also resistant to corrosion deterioration. For each tsunami shelter, safety is examined from several other viewpoints such as air tightness and oxygen concentration. Furthermore, some of companies conducted a water fall test and floating test in the sea. Concerning a form, the product "HIKARi" in Table 1 is an assembling type which is carried in with each part split apart. After being carried into home, they have to put parts together into spherical form and keep it in balcony in its development state. On the other hand, as a tsunami pod which can be kept in foldable state and developed instantaneously in case of emergency, we develop a triangulated ellipsoid body which can be folded by pushing in one direction. This folding way for a sphere has already been researched in [**5, 11**]. Here, we should elucidate the mechanism which makes it possible to deploy a developed ellipsoid body in case of emergency and fold for being stored after use. However, in this paper as the first report, we assume that there is no influence on strength by being deployed and folded. We set its size as 1200 mm of radius for major axis and 800 mm of radius for minor axis and examine the case where one occupant boards a shelter.

2.2. Mathematical modeling for origami pod

The model of tsunami pod in the previous paper [**4**] is generated by calculating coordinates of an ellipsoid approximately, and it can not be folded flatly. In this paper, as a new model of tsunami pod, we develop a triangulated ellipsoid which can be folded flatly. This triangulated ellipsoid does not have strain in the deployed state and the folded state. However, there is strain in the middle of deformation. This structure is often called the "bi-stability" in [**2**].

The following steps give a design method of a triangulated ellipsoid. Let (x_0, y_0, z_0) be a vertex of the the upper-half part of this ellipsoid ($z \geq 0$). In this design method, we define a vertex of the lower-half part ($z \leq 0$) as $(x_0, -y_0, -z_0)$. Thus we may consider the upper-half part of this ellipsoid. In the following (iv), the lower-half part is determined by the position of vertices of the upper-half part. Also we adopt the reversed spiral structure.

(i) Consider an ellipsoid written by the equation $\frac{x^2+y^2}{a^2} + \frac{z^2}{b^2} = 1$, where $a, b > 0$. As a representation by the polar coordinates, we rewrite the above equation as $x = a\cos\theta\cos\varphi$, $y = a\sin\theta\cos\varphi$, $z = b\sin\varphi$, where θ and φ are the latitude and the longitude, respectively.

(ii) Separate this ellipsoid by m planes which is parallel for the xy plane. Let P_k ($k = 0, 1, 2, \cdots, m-1$) be the boundary of a cross-section of this ellipsoid. Here we choose the boundary written as follows.

$$P_k = \{(x, y, z) \mid x^2 + y^2 = r_k^2, \ z = h_k\}, \tag{1}$$

where

$$r_k = \frac{ab}{\sqrt{b^2 + a^2 \tan^2(\frac{k\pi}{2m})}}, \; h_k = \frac{ab\tan(\frac{k\pi}{2m})}{\sqrt{b^2 + a^2 \tan^2(\frac{k\pi}{2m})}}. \tag{2}$$

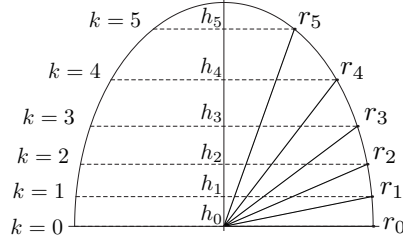Figure 1 shows a graphical image of cross-sections for the side view.

Figure 1. A graphical image of cross-sections for the side view. The parameters are $a = 800$, $b = 1200$, $m = 6$.

(iii) Replace the boundaries of the cross-sections P_k with similar n-sided regular polygons, where n is a natural number which is greater than or equal to 3. Suppose that each vertex is written by

$$U_{j,k} = (x_{j,k}, y_{j,k}, z_{j,k}) \; (j = 0, 1, 2, \cdots, n-1), \tag{3}$$

$$x_{j,k} = r_k \cos\left(\frac{2\pi j}{n} + \sum_{i=0}^{k}\theta_i\right), \; y_{j,k} = r_k \sin\left(\frac{2\pi j}{n} + \sum_{i=0}^{k}\theta_i\right), \; z_{j,k} = h_k,$$

where we suppose $\theta_0 = 0$ for simplicity, and $\theta_k \in \mathbb{R}$ $(k = 1, 2, \cdots, m-1)$. If the inequality

$$0 < h_k - h_{k-1} < 2\sqrt{r_k r_{k-1} \cos\left(\frac{\pi}{n}\right)} \tag{4}$$

holds, then θ_k is determined explicitly. In this design method, we define the following formula of θ_k:

$$\theta_k := (-1)^k \arccos\left(\frac{(h_k - h_{k-1})^2}{4r_k r_{k-1}} + (-1)^{k+1}\sqrt{1 - \frac{(h_k - h_{k-1})^4}{16r_k^2 r_{k-1}^2 \cos^2(\frac{\pi}{n})}} \sin\left(\frac{\pi}{n}\right)\right). \tag{5}$$

Thus triangular faces of the upper-half part of this ellipsoid are given by

$$\triangle U_{j,k-1}U_{j+1,k-1}U_{j,k} \text{ and } \triangle U_{j+1,k-1}U_{j,k}U_{j+1,k} \tag{6}$$

for $j = 0, 1, 2, \cdots, n-1$ and $k = 1, 2, \cdots, m-1$.

(iv) Each vertex of the lower-half part is determined by

$$L_{j,k} = (x_{j,k}, -y_{j,k}, -z_{j,k}). \tag{7}$$

Thus we obtain a triangulated ellipsoid of the lower-half part separated by triangular faces

$$\triangle L_{j,k-1} L_{j+1,k-1} L_{j,k} \text{ and } \triangle L_{j+1,k-1} L_{j,k} L_{j+1,k} \tag{8}$$

for $j = 0, 1, 2, \cdots, n-1$ and $k = 1, 2, \cdots, m-1$.

Throughout the above steps, we can obtain a triangulated ellipsoid, where the top face and the bottom face are a same n-sided regular polygon. Figure 2 shows an example of a triangulated ellipsoid determined by the parameters $a = 800$, $b = 1200$, $n = 10$, $m = 6$. Figure 3 shows origami parts for Figure 2 and its pictures. Each origami part is obtained by applying the design method of [**12**].
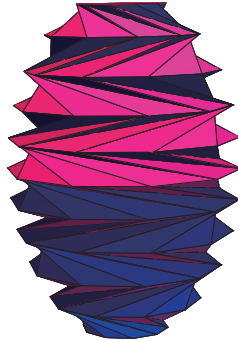

Figure 2. A triangulated ellipsoid. The parameters are $a = 800$, $b = 1200$, $n = 10$, $m = 6$.

2.3. Mathematical modeling for pod and occupant

Since the coordinates of the tsunami pod have already determined for the parameters a, b, m and n, we can obtain a finite element model by quadrilateral mesh shown in Figure 4(a). We apply the 5th percentile adult female among GEBOD Dummy Model shown as in the first right side of Figure 4(b) (LANCEMORE Corporation) developed in the airplane industry, because elder people and disabled people are assumed as an occupant. The model for tsunami pod made in the process mentioned as above is called the initial model without occupant restraint system in the following of this paper. The number of nodes and elements for each part of a pod, a rigid wall, and seawater (tsunami) are shown as in the Table 2. The
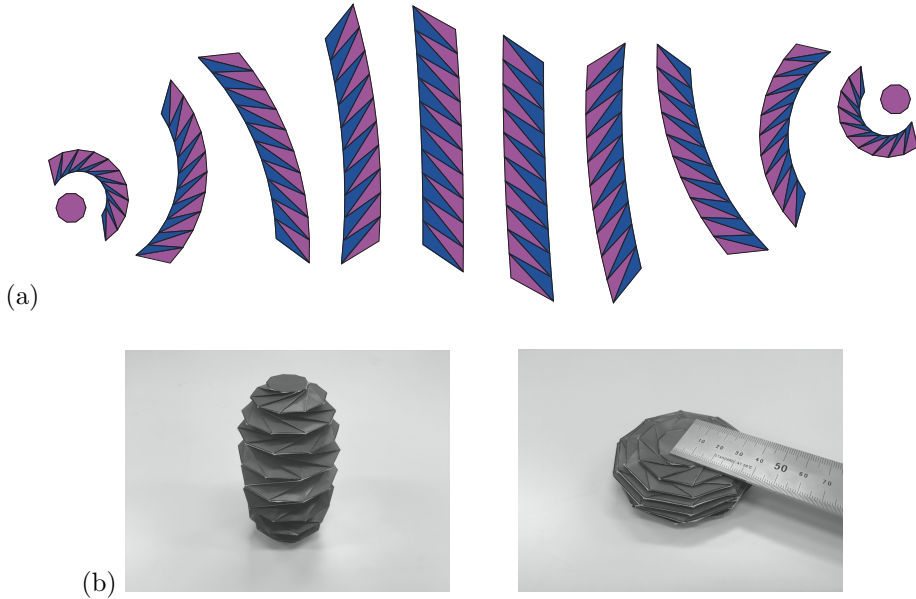
(a)

(b)

Figure 3. (a) Origami parts for Figure 2. (b) Side view of an origami ellipsoid of (a). This can be folded by pushing z-axis direction.

total number for the dummy system is 36138 which are divided into 1636 for shell elements and 2648 for solid ones. The model which a laid occupant is imported into is shown as in the Figure 4(c).

Next, each part is divided into meshes for structure analysis. The way of mesh division is as follows; firstly each side composing a triangle is divided into 5, next those nodes are connected into square meshes regularly and triangle meshes in the case of including a key mode. And, the part of a rigid wall constructed of shell elements is divided into tetrahedron mesh, while the part of seawater constructed of solid elements in 400 times as large as a pod is divided into tetrahedron mesh shown as in Figure 5. The total process for simulation is from the moment when seawater (tsunami) shown as the right panel in Figure 5 starts flowing at an initial constant velocity to the moment when a pod rises onto a wall shown as in the left panel in Figure 5 after hitting on it.

2.4. Analysis theory: fluid-structure coupling analysis

In numerical simulation, we use the software "LS-DYNA" (LSTC Corp., 2014) which is a general-purpose finite element program capable of simulating complex real world problem. This numerical simulation is categorized as fluid structured coupling analysis where a fluid force transform a structure of pod and as well as a transformed structure influences a flow field. In this work, seawater and air are set
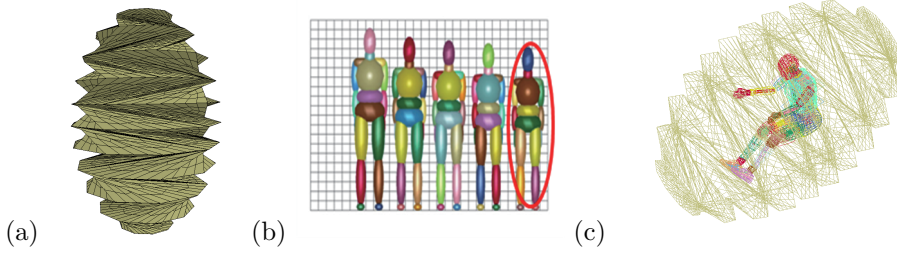
Figure 4. (a) A tsunami pod with quadrilateral mesh. (b) GEBOD Dummy models. (c) A model implemented with a dummy model.
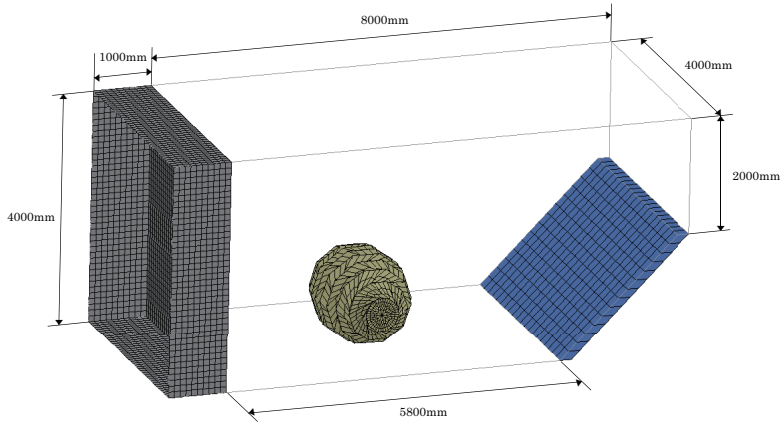

Figure 5. Whole model for simulation including a pod, tsunami, and a rigid wall.

as fluid part, while tsunami pod is set as structured part. Those fluid parts are expressed in the Arbitrary Lagrangian Eulerian (ALE) method, and those structured parts are expressed in coordinate system. The ALE method is to solve simultaneously the conservation rules of mass, momentum, and energy. Each conservation rules are formally written as (9), (10) and (11).

$$\frac{\partial \rho}{\partial t} + \rho \, \mathrm{div}(\boldsymbol{v}) + (\boldsymbol{v} - \boldsymbol{w}) \cdot \mathrm{grad}(\rho) = 0, \tag{9}$$

$$\rho \frac{\partial \boldsymbol{v}}{\partial t} + \rho(\boldsymbol{v} - \boldsymbol{w}) \cdot \mathrm{grad}(\boldsymbol{v}) = \mathrm{div}(\boldsymbol{\sigma}) + \boldsymbol{f}, \tag{10}$$

$$\rho \frac{\partial \boldsymbol{e}}{\partial t} + \rho(\boldsymbol{v} - \boldsymbol{w}) \cdot \mathrm{grad}(\boldsymbol{e}) = \boldsymbol{\sigma} : \boldsymbol{D} + \boldsymbol{f} \cdot \boldsymbol{v}. \tag{11}$$

Part	Element type	The number of elements	The number of nodes
Pod	Shell	4960	4957
Wall	Shell	3200	3281
Seawater (Tsunami)	Solid	18240	20454
Dummy model	Shell / Solid	1636 / 2648	7446
Total number		26400	36138

Table 2. Details for a whole model.

where ρ is fluid density, $\boldsymbol{v}$ is velocity vector of fluid, $\boldsymbol{w}$ is velocity vector of mesh, $\boldsymbol{e}$ is energy per unit mass, $\boldsymbol{\sigma}$ is Cauchy stress tensor, $\boldsymbol{D}$ is deformation velocity tensor, $\boldsymbol{f}$ is body force. In numerical simulation, seawater (fluid part) shown as in Figure 6(a) touches tsunami pod (structured part), and then the mesh of seawater and air are deformed internally (Figure 6(b)), and finally the mesh is restored to the initial position (Figure 6(c)). In this procession, the advection term including $\boldsymbol{v} - \boldsymbol{w}$ in (11) is calculated [1].
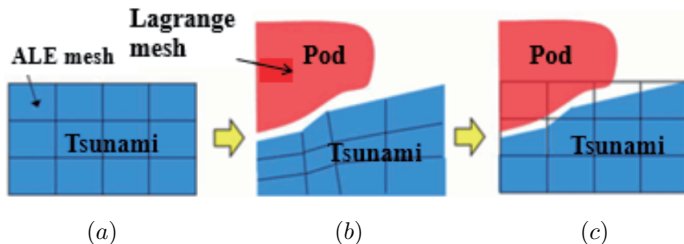

Figure 6. The Arbitrary Lagrangian and Eulerian (ALE) method. (a) Initial mesh. (b) Deformed internal mesh. (c) Mesh restored to the initial position.

The applied penalty method generally used in the contact calculation for structure analysis is applied into coupling calculation method with structured part (pod) and fluid (tsunami). As shown in Figure 7, those contact points are placed on the contact positions with structure part and fluid one. The contact points are shifted following to the fluid transfer, however the virtual spring between the transferred point and the former one is generated. The force exerted by the extended spring expresses the pressure which a structure is exerted by fluid. The spring stiffness k for the virtual string is given as (12).

$$k = p_f \frac{KA^2}{V}, \tag{12}$$

where K is a volume modulus for a fluid element, A is average area for a structure element, V is a volume for a fluid element, p_f is scale factor [1]. On this condition,

the force P which the structure body receives is expressed as (13).

$$P = kd, \tag{13}$$

where d is intrusion of fluid into structure body. This coupling method has short time steps for an explicit method, therefore intrusion into fluid for 1 step is a little.
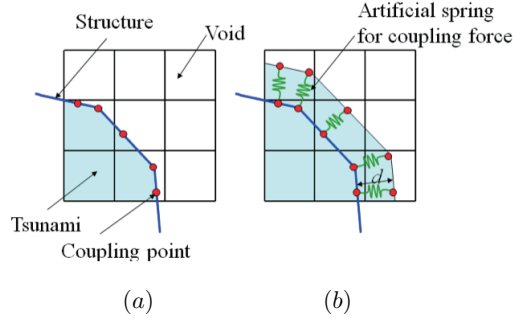

Figure 7. Fluid structure coupling procedure using penalty based method. (a) Initial configuration. (b) Generation of artificial spring at the next step.

2.5. Conditions for simulation and video image shots

CFRP applied into a pod is compound material which has a layered structure. As a product specification for a commercial CFRP, a tensile strength and a bending stress (nominal stress) are mentioned. Therefore, in this paper, a pod is dealt as a simple elastic body, and the load provided on its structure is estimated by von Mises stress to compare with the strength of an actual product. The thickness of a tsunami pod in simulation is set as 4.0 mm which is the minimum among the products. The properties for CFRP as material are as follows; Young's modulus is 294 GPa, Poisson's ratio is 0.12, and density is 1.8×10^{-9} ton/mm^3. A tsunami velocity is calculated as follows. A tsunami velocity in transmitting on the sea is in proportion to the root of sea depth, however a tsunami velocity we apply into simulation is the one after flowing into the land which is slower than to the one on the sea , because there are factors of reducing velocity that depth is lower and there are obstacles. The velocity for simulation is calculated as 8 km/sec by the distance which certain object move for a given period in the video taken in the Tohoku earthquake. Figure 8 shows video image shots in numerical simulation from the moment tsunami touches a pod to the moment the tsunami pod rises onto the wall. In the latter process of this numerical simulation, an occupant hits on the internal wall of a tsunami pod to be injured possibly. For preventing that, we try to reinforce an occupant with an occupant reinforcement system similar to a safety bar applied into roller coaster. In the next section, the strength of a tsunami pod

and the injury degree of an occupant are compared between the model without a
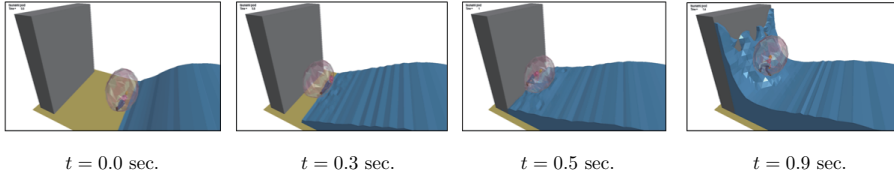reinforcement and the one with it.

<div align="center">
$t = 0.0$ sec. $t = 0.3$ sec. $t = 0.5$ sec. $t = 0.9$ sec.
</div>

Figure 8. Video image shots in numerical simulation.

3.   Analysis result of numerical simulation

3.1.   Strength confirmation of the initial model without an occupant restraint system

Firstly, strength is verified in case of the initial model without an occupant re-
inforcement system. It would be evaluated as not satisfying safety, if any elements
of a pod exceeded von Mises equivalent stress for CFRP $(500 - 1500$ MPa$)$. As
a result of the numerical simulation, the maximum of von Mises equivalent stress
value among each element (written shortly as Maximum Mises stress in the follow-
ing sentences) is 1272 as illustrated in Figure 9, it is judged that a pod may be
deformed or broken.
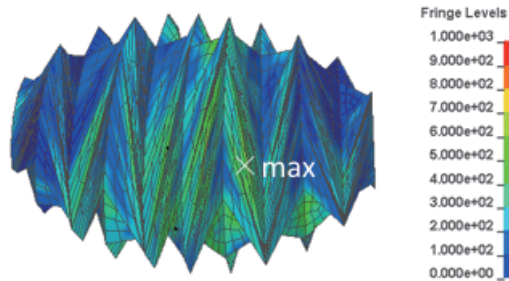
Figure 9. Color contour for the maximum of von Mises equivalent stress
at the moment that a resultant force become maximum in case of the
initial model without an occupant restraint system.

3.2.   Confirmation of Head Injury Criterion for the initial model

Head Injury Criterion (HIC) is a measure of the likelihood of head injury aris-
ing from an impact. HIC is calculated by (14) using head acceleration and its
duration. A big acceleration value for a short duration period is allowed, because
the calculated HIC value is an average of every 0.036 seconds. The value below

1000 is judged as safe where 1 of 6 people suffer a critical injury in the brain. The time transformation of HIC in case of the initial model is shown as in Figure 10. It is proved that the value calculated by (14) is 8142 which is around 8 times as the safety level 1000, therefore it is likely that an occupant would be seriously damaged.
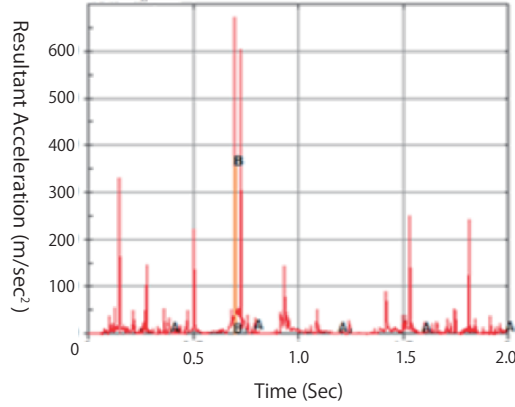

Figure 10. Resultant acceleration for the head of an occupant in case of the initial model without an occupant restraint system.

$$\text{HIC} = \left\{ \left[\frac{1}{t_2 - t_1} \int_{t_1}^{t_2} a(t) \, dt \right]^{2.5} (t_2 - t_1) \right\}_{\max}, \tag{14}$$

where t_1 and t_2 indicate the initial and final times (seconds) and a indicates acceleration. Here we suppose that $[t_2 - t_1] \leq 0.036$s.

3.3. Strength confirmation of the modified model with an occupant reinforcement system and its HIC value

It is confirmed from the video image shots as above that an occupant is rotating violently and then hits on the internal side of a pod, finally is injured in the head severely. For an automobile, 4-point or 5-point seat belts are adopted to respond to front collision, the reinforcement to fix an upper body and a lower body separately which imitates the safety bars of a roller coaster is designed as Figure 11. Then, is implemented with the designed bars, the seat, and a dummy model whose positions are arranged whose position is arranged not to contact with other parts as Figure 11(b). This model is called model with an occupant restraint system in the following. The parts of a seat and a reinforcement are integrated with a pod to be defined as a rigid body consisting of 5914 nodes and 5858 shell elements totally. The thickness of an outer wall is increased from 4.0 mm in case of the initial model

to 6.0 mm for strengthening its structure. As a result of the numerical simulation in case of the modified model with an occupant reinforcement system, maximum Mises stress in some elements of a pod in collision is 789 MPa which is less than the strength of CFRP(500 − 1500 MPa) and the condition for damage failed to be improved shown as in Figure 12. On the other hand, HIC value is decreased by more than 90% to become 76 in value shown as in Figure 13 which is well below the safety level 1000.

(a)   (b)
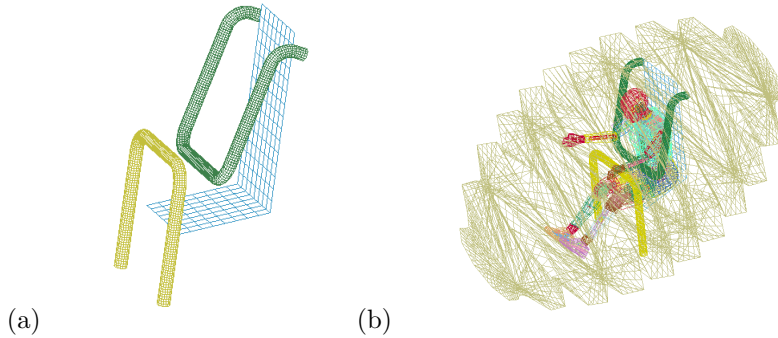
Figure 11. A model with an occupant restraint system. (a) An occupant restraint system. (b) Modified model.

Figure 12. Color contour for the maximum of von Mises equivalent stress at the moment that a resultant force become maximum in case of the model with an occupant restraint system.

4. Optimization of structure of tsunami pod

4.1. Conditions for optimization

By applying the modified model with a reinforcement, the following optimization is attempted. Those ranges for each design variable are as follows:

Figure 13. Resultant acceleration for the head of an occupant in case of the model with an occupant restraint system.

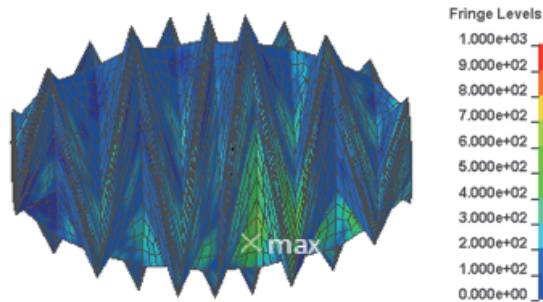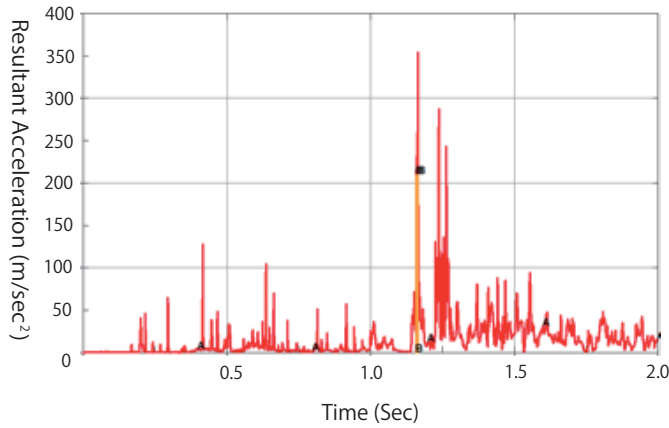$900 <$ major axis$(a) < 1320$, $600 <$ minor axis$(b) < 880$, $2.0 <$ thickness$(t) < 6.0$, $345 <$ Young's modulus$(E) < 450$. Here, HIC is excluded from consideration, because it has already satisfied safety in the result of the simulation applying the modified model with a reinforcement. Under the above conditions, each design variables are calculated to minimize the mass of a pod. The velocity is set as constant 4 m/sec in the x axis. For shortening a calculation time, a dummy model is set as rigid body, and apply decoupling analysis in optimization, and later the validity of the obtained optimal model is verified by coupling analysis. Incidentally, the calculation time for 1 step in decoupling analysis is one half as short as the one in coupling analysis. We use a software named LS-OPT [1] applying Radial Basic Function (RBF) as response surface function. Initially, 5 sample points are input and an optimum solution is searched while generating response surfaces of a objective function and a constraint function by RBF network. The condition of finishing a calculation is the case where the relationship of optimal value obtained this step and the one obtained in the last step. If (15) is not satisfied, 5 sample points are added.

$$\frac{[\text{optimal value obtained in this step} - \text{optimal value obtained in the last step}]}{[\text{optimal value obtained in this step}]} \leq 0.01. \tag{15}$$

4.2. Result of optimization

Firstly, we check the correlation between each design value, objective values and the value of constraint condition as in the Table 4. It is found that mass of pod is

Design value	
Major axis (mm)	$900 < a < 1320$
Minor axis (mm)	$600 < b < 880$
Thickness (mm)	$2.0 < t < 6.0$
Young's modulus (GPa)	$345 < E < 450$
Objective function	
Minimizing the mass of pod (kg)	
Constraint condition[*]	
Maximizing von Mises equivalent stress (MPa) for each element is less than the strength for CFRP	

Table 3. The range of design value, objective function and constraint condition. In this table, the mark ∗ implies that HIC is excluded.

higher positive correlated with a major axis and a minor axis than with thickness and Young's modulus, so it is necessary to reduce a size for making the model of a pod light-weighted. And, also it is found that thickness needs to be smaller and Young's modules needs to be lower. While the maximum Mises stress as constraint condition has a higher negative correlation with major axis and minor axis than Young's modules, and little correlated to thickness. It can be said for minimizing the maximum Mises stress it is necessary to increase a size and Young's modules. Therefore, as a result of the above consideration, optimization is predicted to be under unstable process in changing the size while arranging thickness and Young's modules.

The relationships are illustrated as in Figure 14 (a), (b) and (c) drawn by a software for optimization "LS-OPT" with an interface to LS-DYNA. These make it easier to understand the relationship as mentioned above visually.

		Variables				Response	
		Major axis (mm)	Minor axis (mm)	Thickness (mm)	Young's modulus (GPa)	Mass (kg)	Maximum Mises (MPa)
Variables	Major axis (mm)	-	0.97	-0.17	0.29	0.83	-0.90
	Minor axis (mm)	-	-	-0.16	0.29	0.88	-0.90
	Thickness (mm)	-	-	-	-0.07	0.16	0.05
	Young's modulus (GPa)	-	-	-	-	0.23	-0.17
Response	Mass (kg)	-	-	-	-	-	-0.76
	Maximum Mises (MPa)	-	-	-	-	-	-

Table 4. The values of correlation coefficient between variables.
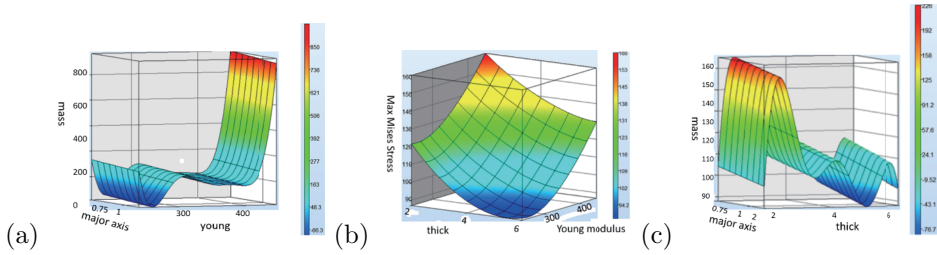
(a)   (b)   (c)

Figure 14. Visualized color charts for correlation between design values, objective function and constraint condition.

The result of optimization process is shown as in Table 5 which illustrates those pod images during optimization process from time step 1 to 6. The calculation takes 5 days to run from step 1 to step 6. And, in checking the result, the optimization of size is converged in the 4th step, and after that thickness and Young's modules are made to be converged until 6th step. The comparison between the optimal model from 6th step and the initial model is shown as in Table 6.

times of roop	a (scale)	a(actual)	b (scale)	b(actual)	t (mm)	Young's modulus (GPa)	mass (kg)	constraint condition(max vonmises(MPa))	image of model
1	1.00	1205	0.75	600	4.3	240	132	163	
2	0.97	1164	0.84	668	2.7	240	100	91	
3	0.98	1176	0.76	608	4.6	323	140	83	
4	1.10	1320	0.75	600	5.5	301	233	105	
5	1.10	1320	0.75	600	6.0	285	440	87	
6	1.10	1320	0.75	600	5.1	323	153	96	

Table 5. Optimization process from time step 1 to 6.

	Initial value	Optimal value
Design value		
Major axis (mm)	1.0	1.1
Minor axis (mm)	1.0	0.75
Thickness (mm)	6.0	5.1
Young's modulus (GPa)	294	323
Objective function		
mass (kg)	297	153
Constraint condition		
The Maximum of von Mises equivalent stress (MPa)	789	96

Table 6. Comparison between the initial values before optimization and the optimal values after optimization.

References

[1]   LS-DYNA KEYWORD USER'S MANUAL VOL. I - III, LIVERMORE SOFTWARE TECHNOLOGY CORPOTATION (LSTC Corp.) (2014).

[2]   Ishida, S., Uchida, H., and Hagiwara, I., Vibration isolators using nonlinear spring characteristics of origami-based foldable structures, Bulletin of the JSME, Vol. 80, No. 820 (2014) (in Japanese).

[3]   Mitsume, N., Yoshimura, S. and Murotani, K., Fluid-structure coupled analysis using finite element method and particle method, Proceedings of computational engineering and science, Vol. 17, B-4-2 (2012) (in Japanese).

[4]   Nakayama, E., Nguyen, H., Tokura, S. and Hagiwara, I., Modelling and simulation for optimal design of foldable tsunami pod, Transactions of the Japan Society of Mechanical Engineering, Vol. 81, No. 829 (2015) (in Japanese).

[5]   Nojima, T., Modelling of Folding Patterns in Flat Membranes and Cylinders by Using Origami, Transactions of the Japan Society of Mechanical Engineers, Series. C, Vol. 66, No. 643 (2000), pp.1050–1056 (in Japanese).

[6]   SANKYO MANUFACTURING Co.,Ltd. ＞ CFRP ＞ Data collection for performance comparison (online), available from `http://www.sankyo-ss.co.jp/about-cfrp/performance.html`, (accessed on 15 May, 2015) (in Japanese).

[7]   Shigematsu, T., Akechi, K. and Koike, T., Basic experiment about the development of a float typed tsunami shelter, Journal of civil engineering in the ocean, Vol. 24 (2008), pp.105–110 (in Japanese).

[8]   Shigematsu, T. and Nakahigashi, D., Experimental research about the motion property of double float typed tsunami shelter, Journal of civil engineering, B2 Coastal engineering, Vol. 67, No. 2 (2011), pp.751–755 (in Japanese).

[9]   Souli, M., Ouahsine, A. and Lewin, L., Arbitrary Lagrangian Eulerian Formulation for Fluid-Structure Interaction Problems, Computer Methods in Applied Mechanics and Engineering, Vol. 190 (2000), pp. 659–675.

[10] Stander, N., Willem, R. and Goel, T., Eggeleston. and Craig, K, LS-OPT user's manual design optimization and probabilistic analysis tool for the engineering analyst, Livermore software technology corporation, Ver. 4.2 (2012).

[11] Sugiyama, F. and Nojima, T., Development of folding method of spherical membrane in both radial and axial directions, Transactions of the JSME, Vol. 80, No. 814 (2014) (in Japanese).

[12] Sushida, T., Hizume, A. and Yamagishi, Y., Design methods of origami tessellations for triangular spiral multiple tilings, Origami[6]: I. Mathematics (2015), pp. 241–251.

Eri Nakayama

Graduate School of Advanced Mathematical Sciences, Meiji University
811, 4-21-1, Nakano, Nakano-ku, Tokyo 164-8525, Japan
tz12007@meiji.ac.jp

Takamichi Sushida

Meiji Institute for Advanced Study of Mathematical Science, Meiji University
809, 4-21-1, Nakano, Nakano-ku, Tokyo 164-8525, Japan
tz14024@meiji.ac.jp

Ichiro Hagiwara

Meiji Institute for Advanced Study of Mathematical Science, Meiji University
811, 4-21-1, Nakano, Nakano-ku, Tokyo 164-8525, Japan
ihagi@meiji.ac.jp